ELSEVIER

Journal of Photochemistry and Photobiology A: Chemistry 104 (1997) 141–149

Journal of PHOTOCHEMISTRY AND PHOTOBIOLOGY A:CHEMISTRY

Quenching of chlorophyll *a* fluorescence by oxygen in highly concentrated solutions and microdroplets

Keiji Nakamura, Takashi Kowaki, Andrew D. Scully [1], Satoshi Hirayama *

Laboratory of Chemistry, Kyoto Institute of Technology, Matsugasaki, Sakyo-ku, Kyoto 606, Japan

Received 3 September 1996; accepted 11 December 1996

Abstract

The quenching of chlorophyll *a* (Chl *a*) fluorescence by oxygen was studied using bulk solutions and microdroplets of *n*-octanol over a Chl *a* concentration range of 0.1 μM to 82 mM. Chl *a* exhibits significant self-quenching (concentration quenching) over this concentration range. The technique of time-resolved fluorescence microscopy was employed to remove the effects of re-absorption. The fluorescence decay curves measured for both aerated and deaerated bulk solutions can be described satisfactorily by a single-exponential function when the concentration of Chl *a* is not higher than 50 mM. The value of the net rate constant for the fluorescence quenching by oxygen in the bulk solutions (k_q) shows a distinct dependence on the Chl *a* concentration for concentrations higher than 1 mM, and reaches a value of $(2.0 \pm 0.5) \times 10^{10}\ M^{-1}\ s^{-1}$ at 25 mM. This value of k_q is approximately five times larger than that obtained for the most dilute bulk solution. The fluorescence decay curves measured for Chl *a* in deaerated droplets are approximately exponential, but photodegradation in the aerated droplets is so significant that the fluorescence decays cannot be described by a single-exponential function. Instead, a sum of two exponentials is required, with the longer lived component being attributed to the quenched fluorescence from Chl *a*. The values of both the quenched and unquenched fluorescence lifetimes decrease with decreasing droplet size, and the net rate constant for the fluorescence quenching by oxygen in the microdroplets (k_q^D) is dependent not only on the concentration of Chl *a* but also on the size of the droplet. The largest value for k_q^D of $(85 \pm 12) \times 10^{10}\ M^{-1}\ s^{-1}$ was found in a 4 μm droplet at a Chl *a* concentration of 30 mM. This droplet size dependence of the fluorescence quenching by oxygen is ascribed mainly to enhanced energy migration in the smaller droplets, which results in an effective increase in the quenching radius of oxygen. © 1997 Elsevier Science S.A.

Keywords: Chlorophyll *a*; Concentration effect; Droplet; Energy migration; Fluorescence quenching by oxygen; Size effect

1. Introduction

The oxygen molecule is unique in that it quenches most molecules in their electronically excited singlet, triplet, excimer or exciplex states [1]. The efficiency of quenching of these electronic states is so high that the quenching reactions by oxygen in solution are often believed to occur at the diffusion-controlled reaction rate [2]. However, this is not always the case. As demonstrated previously [3–5], the excited singlet state of some anthracene derivatives is quenched by oxygen at a rate which is significantly slower than the rate of diffusion. The mechanism and rate of quenching by oxygen appear to vary from molecule to molecule, being influenced by various factors, such as the solvent viscosity, solvent polarity, fluorophore concentration and spatial heterogeneity. Quenching of the fluorescence from chlorophylls by oxygen is of particular interest because chlorophylls play a key role in photosynthesis, being present in spatially confined photosynthetic organelles at very high concentrations under aerobic conditions [6].

The migration of the absorbed electronic excitation energy in highly concentrated solutions is affected by re-absorption, energy transfer and the formation of dimers and/or higher aggregates which can act as quenching traps for the migrating excitation energy [7–9]. Therefore the quenching of fluorescence by oxygen is usually studied using dilute solutions in order to avoid the complications caused by increasing fluorophore concentration. The effects of quenching by oxygen in studies of self-quenching of fluorescence are often neglected. Studies of the photodynamics of chlorophylls in vivo often fail to include any evaluation of the consequences of the presence of oxygen [6] on the photophysical and photochemical behaviour of the chlorophyll molecules which exist in chloroplasts (which have an approximate hemispherical geometry with a typical diameter of 5 μm [10]) at local

* Corresponding author. Tel.: +81 75 724 7743; fax: +81 75 724 7710.

[1] Present address: Central Laser Facility, Rutherford Appleton Laboratory, Chilton, Didcot, Oxon. OX11 0QX, UK.

PII S1010-6030(97)04612-6

concentrations of the order of 10–100 mM [11]. Consequently, the following two issues were addressed in this work:

1. the extent to which the process of fluorescence quenching by oxygen is influenced by energy migration occurring in highly concentrated solutions;
2. the determination of whether or not the quenching process is affected by the size of the space in which the chlorophyll and oxygen molecules are confined.

2. Experimental section

The experimental details of the fluorescence decay measurements using time-resolved fluorescence microscopy are the same as those described previously [8,12–14]. The excitation source was a mode-locked Spectra Physics model 2016 Ar^+ ion laser operating at 514.5 nm. Chlorophyll *a* (Chl *a*) photodegrades more readily in aerated solutions [15] than in deaerated solutions. The extent of photodegradation is even more drastic in aerated droplets. Therefore, in order to minimize the photodegradation caused by laser irradiation, the number of counts in the channel of maximum intensity of the fluorescence decay curves measured for the microdroplets was kept to 2×10^3 or less. The fluorescence emission was detected using a Hamamatsu R928 photomultiplier tube mounted on the camera port of the fluorescence microscope (Nikon XF-EFD) after transmission through a Toshiba O-54 glass cut-off filter inserted before the photomultiplier to remove any scattered excitation light. The diameter of the illuminated spot was less than 10 μm. The laser excitation intensity at the sample was measured with a Newport model 835 power meter to be less than 2 μW, which was sufficiently low so as to avoid lasing in the droplets. The "magic angle" for the microscope system was determined experimentally by measuring the fluorescence decay from a thin liquid film of a dilute ethylene glycol solution of rhodamine 6G (R6G) sandwiched between a coverslip and a microscope slide and by adjusting the orientation of the probe polarizer until an exponential decay was recovered [8,13,14]. All of the fluorescence decay curves have a channel width of 20.9 ps.

Aerated microdroplets of *n*-octanol were prepared by dispersing an air-saturated *n*-octanol solution of Chl *a* in water. A small amount of the upper layer containing the smaller droplets was sucked into a glass capillary of approximately 100 μm inner diameter. Both ends of the glass capillary were sealed with compound rubber prior to being mounted on the stage of the fluorescence microscope for the fluorescence decay measurements.

Deaerated droplets were prepared by mixing a deaerated *n*-octanol solution of Chl *a* with deaerated water in vacuum. To achieve this, an H-shaped cell with a glass capillary side arm was used, as described previously [13]. Droplets dispersed in water were introduced into the capillary side arm and an appropriate droplet was selected under the microscope. Droplet sizes were measured using an objective micrometer. The uncertainty associated with the diameter measurements was estimated to be approximately 25% for the droplets of the smallest size.

Distilled water and *n*-octanol (guaranteed grade, Wako Pure Chemical Industries Ltd.) were used as received. The other organic solvents were of spectroscopic grade. The organic solvents used in this work were not treated to remove traces of water. The bulk sample solutions were degassed by several repeated freeze–pump–thaw cycles. Chl *a* extracted from *Spirulina* (Wako Pure Chemical Industries Ltd.) was used without further purification. This source of Chl *a* yielded several peaks on high performance liquid chromatography (HPLC) (silica-1151-N; *n*-hexane–isopropanol (98.4:1.4); monitored at 430 nm) which were ascribed to a number of chlorophyll derivatives. However, the peak assigned to Chl *a* accounts for 98% of the total peak intensity.

The absorption spectra of highly concentrated solutions of Chl *a* were measured using a Shimadzu A207 spectrophotometer. The solutions were contained in a home-built thin cell consisting of two optical quartz plates (50 mm × 30 mm × 3 mm). The two quartz plates were pressed together by springs at the four corners of a metal holder [16,17]. The effective path length of the optical cell was approximately 10 μm. The absorption spectra of Chl *a* at concentrations of the order of 10 mM could be measured using this cell. The fluorescence spectra of dilute solutions were recorded using a Shimadzu RF 502 spectrofluorophotometer. A Nikon XF-EFD epi-illumination fluorescence microscope, fitted with a Hamamatsu C2327 PCD photodetector (1024 channels) operating at −20 °C, was used to record the fluorescence spectra of concentrated solutions in a manner similar to that reported previously [18]. All of the kinetic and spectral measurements were performed at room temperature. Oxygen concentrations in solution were determined by gas chromatography (molecular sieve 5 Å), when no literature values were available [3,19]. The water content in the *n*-octanol droplets dispersed in water was determined to be approximately 5% by volume using gas chromatography (Polapack Type Q).

3. Results and discussion

3.1. Concentration quenching of Chl *a* fluorescence in bulk solution

The fluorescence from dyes in highly concentrated solutions is often quenched strongly without being accompanied by the appearance of a new emission band. Chlorophylls are a well-known example of such molecules [20,21]. The fluorescence lifetime of Chl *a* in *n*-octanol was measured as a function of concentration using a thin glass capillary to avoid distortion due to the effects of re-absorption [8,12]. The fluorescence decay curves measured at several Chl *a* concentrations are shown in Fig. 1. The full lines through the dots represent the best-fit single-exponential decays, and the corresponding reduced residual distributions are shown in Fig. 2. The fluorescence lifetimes calculated from these decay curves

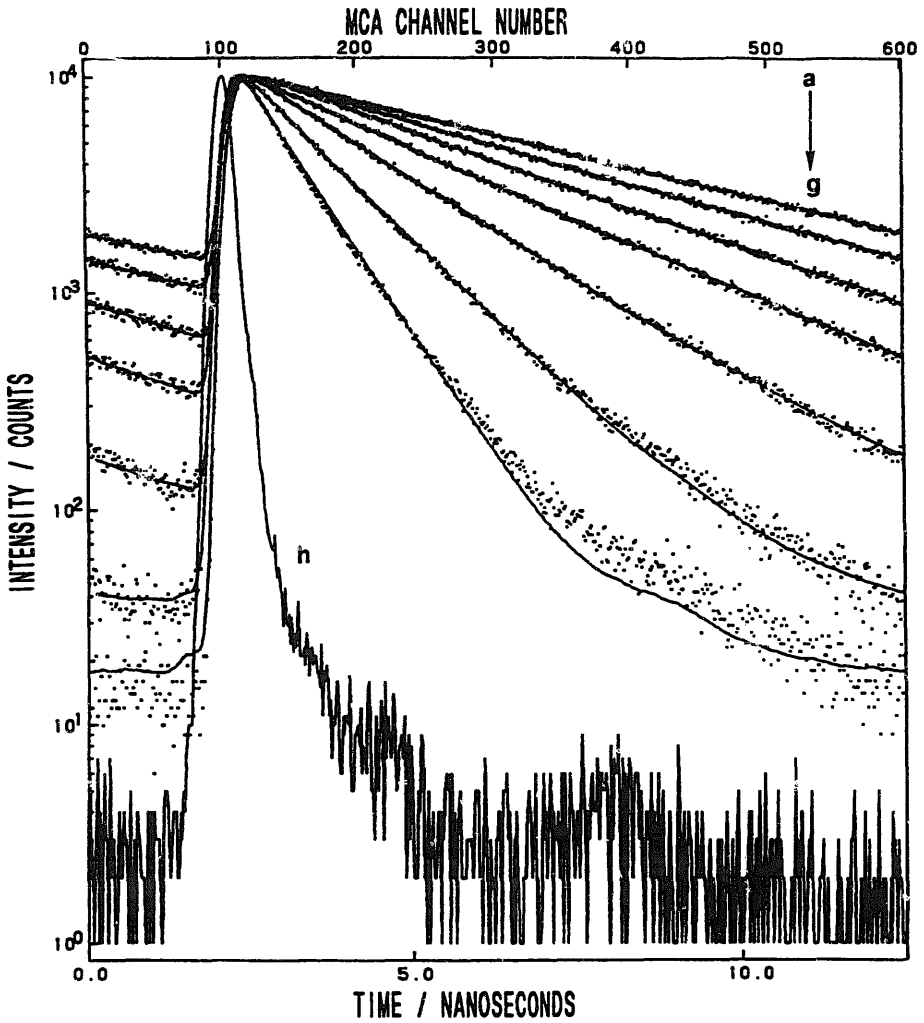

Fig. 1. Fluorescence decay curves (dots) measured for degassed solutions of Chl *a* in *n*-octanol contained in thin glass capillaries. Concentrations of Chl *a*: (a) 1.0 mM; (b) 7.5 mM; (c) 15 mM; (d) 20 mM; (e) 30 mM; (f) 50 mM; (g) 82 mM. Full lines are the best-fit decay curves calculated using a single-exponential function. Curve (h) is the instrument response function.

are plotted in Fig. 3 as a function of the concentration. The fluorescence decay curves measured for Chl *a* at concentrations of less than 1.0 mM can be described satisfactorily by a single-exponential function with a decay time of 5.65 ± 0.04 ns. The fluorescence lifetime displays a systematic decrease when the Chl *a* concentration is increased above 1.0 mM, but the fluorescence decay remains exponential until the Chl *a* concentration reaches 50 mM. At this concentration, the decay curve displays a perceptible deviation from exponentiality. The non-random reduced residual distributions observed for decay curve (g) in the top panel of Fig. 2 illustrates the clear deviation from exponentiality for the decay curve measured at a Chl *a* concentration of 82 mM.

A comparison of the absorption spectra measured for Chl *a* in *n*-octanol at 0.1 μM and 10 mM does not suggest the presence of any new absorption bands, since the relative peak intensities and widths at half-maximum of the major bands located at 433, 620 and 667 nm are found to be the same for the two spectra. The fluorescence emission spectrum displays a peak at 675 nm in dilute *n*-octanol solution (0.1 μM), and no appreciable spectral shift or any new emission bands are observed when the concentration is increased to 10 mM. Although no spectral evidence for the formation of Chl *a* dimers in *n*-octanol has been obtained, an analysis of the fluorescence decay curves obtained for highly concentrated solutions using the Loring–Anderson–Fayer (LAF) model [22] described below enables an estimation to be made of the concentrations of the dimer (or statistical pair [19]) of Chl *a*, and hence the equilibrium constant for dimer formation.

Loring et al. [22] proposed a model to describe the modification to the time dependence of the fluorescence emission which arises as a result of energy migration and subsequent trapping (quenching) of this migrating energy. It was assumed in the development of this model that material diffusion is negligible, back energy transfer from the trap to the donor molecule does not occur and that the trap itself is non-emissive. The fluorescence decays of Chl *a* in concentrated *n*-octanol solutions satisfy these conditions, assuming that the energy migration among the Chl *a* molecules is governed by Förster-type energy transfer [23] and that the dimer behaves as a non-emissive trap.

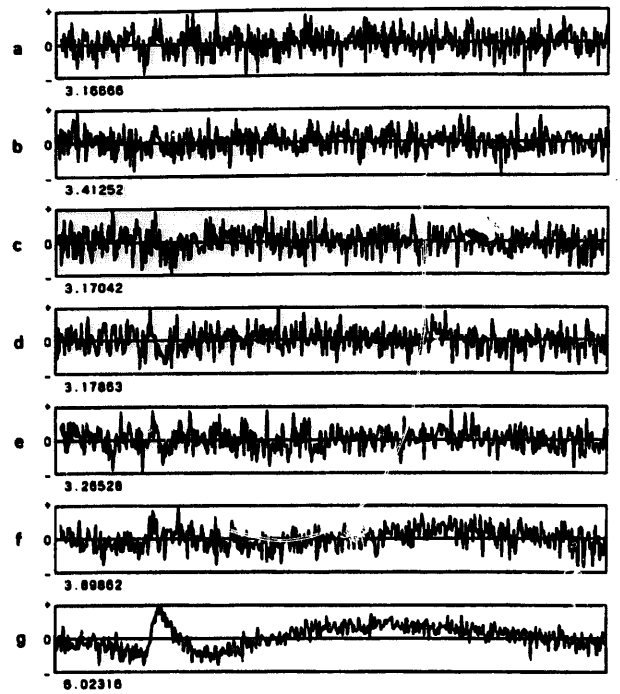

Fig. 2. Distribution of reduced residuals corresponding to the analysis using an exponential function of the fluorescence decay curves shown in Fig. 1. Decay curves (a)–(g) from bottom to top.

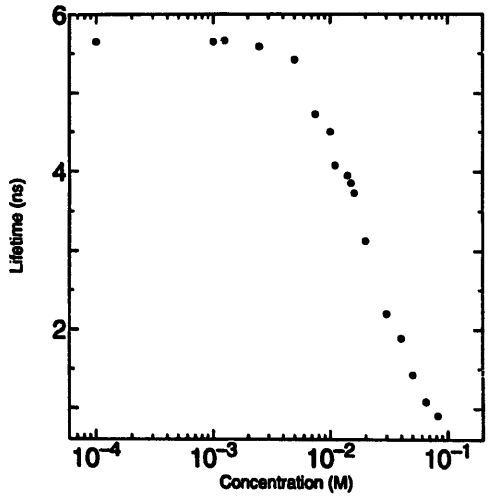

Fig. 3. Plot of the best-fit exponential decay times obtained for Chl *a* in deaerated *n*-octanol solutions as a function of concentration.

The fluorescence decay curves shown in Fig. 1 were analysed using the LAF model [22], with the details of the method of analysis given in Ref. [8]. The model-related parameters used for curve fitting are the critical distance for energy transfer from the monomer to the dimer (R_0^{MD}) and the reduced concentrations of the monomer and dimer, from which the equilibrium constant (K_{MD}) can be calculated. The quality of fitting is satisfactory over the whole concentration range examined, in contrast with the poor fitting of the decay curve (g) in Fig. 1 to a single exponential. However, the values recovered for R_0^{MD} and the values calculated for K_{MD} are constant only up to a Chl *a* concentration of 20 mM. Above this concentration, the values of R_0^{MD} display a systematic decrease with increasing concentration and the values of K_{MD} display a systematic increase. These results imply that higher order aggregates may be formed in significant concentrations at Chl *a* concentrations greater than 20 mM, resulting in the inapplicability of the LAF model. The average best-fit values for R_0^{MD} and K_{MD} over the concentration range 5.0–20 mM are 4.6 ± 0.4 nm and 2.6 ± 0.4 M^{-1} respectively. The value obtained for K_{MD} indicates that the mole fraction of the dimer is less than 0.03 over this concentration range. Such a low fraction of the dimer is consistent with the lack of spectroscopic evidence for dimer formation in *n*-octanol. This behaviour is in contrast with the facile formation of dimers and higher aggregates of Chl *a* in non-polar solvents, such as carbon tetrachloride, for which an abundance of spectroscopic and thermodynamic evidence exists [24].

Although no spectral evidence could be obtained for the formation of Chl *a* dimers in *n*-octanol, the presence of only a minute concentration of dimers would be sufficient to result in considerable quenching of Chl *a* monomer fluorescence if the migration of excitation energy among Chl *a* monomers is very efficient. The efficiency of energy migration can be estimated using the critical distance for energy transfer (R_0^{MM}), defined in Eq. (1), assuming that the transfer of excitation energy proceeds via a Förster-type mechanism

$$(R_0^{MM})^6 = \frac{9000 \ln(10) \kappa^2 \phi_0}{128 \pi^5 n^4 N} \int_0^\infty \frac{F_D(\bar{\nu}) \epsilon_A(\bar{\nu})}{\bar{\nu}^4} d\bar{\nu} \quad (1)$$

where ϕ_0 is the fluorescence quantum yield of the unquenched fluorophore, κ^2 is an orientational factor given by 0.476, $F(\bar{\nu})$ is the spectral distribution of the fluorescence emission in quanta normalized to unity, $\epsilon(\bar{\nu})$ is the decadic molar extinction coefficient at the wavenumber $\bar{\nu}$ and n is the refractive index of the solvent [23]. The probability of an electronically excited Chl *a* monomer decaying radiatively or by non-radiative energy transfer to a neighbouring Chl *a* monomer is equal when the two Chl *a* monomers are separated by a distance of R_0^{MM}. The value of R_0^{MM} for Chl *a* in *n*-octanol was calculated to be 5.2 nm using the absorption and fluorescence spectra measured in this work. The mean separation distance r between the monomers for a solution containing a Chl *a* concentration of 1.0 mM is 7.3 nm. The efficiency of energy transfer $E(r)$ at this concentration is calculated to be 11% using Eq. (2)

$$E(r) = \frac{(R_0^{MM})^6}{(R_0^{MM})^6 + r^6} \quad (2)$$

In contrast, the mean distance between neighbouring monomers at a Chl *a* concentration of 10 mM is 3.4 nm, resulting in a calculated efficiency of energy transfer between Chl *a* monomers of 93%. This value of $E(r)$ will be a slight overestimate of the actual value due to the reduction in monomer concentration occurring as a result of dimer formation. However, the effect of this on the calculated value of $E(r)$ is expected to be negligible considering the very low mole fraction of dimers. It is evident from these simple calculations

Table 1
Rate constants of fluorescence quenching by oxygen for Chl *a* (0.1 μM) in various solvents

Solvent	$[O_2]$ (mM)	η (cP)	τ_0 (ns)	τ_q (ns)	k_q (10^{10} M^{-1} s^{-1})
Methanol	2.12	0.545	5.97±0.05	5.55±0.04	0.60±0.13
Ethanol	2.07	1.708	5.85±0.05	5.50±0.05	0.53±0.15
1-Propanol	2.20	2.004	5.64±0.05	5.32±0.05	0.49±0.15
2-Propanol	2.11	2.130	5.76±0.04	5.46±0.04	0.45±0.12
1-Butanol	1.80	2.640	5.48±0.04	5.25±0.04	0.44±0.16
n-Pentanol	1.90	3.347	5.43±0.05	5.20±0.04	0.43±0.17
2-Methyl-1-propanol	1.77	3.910	5.68±0.05	5.40±0.05	0.52±0.18
n-Octanol	1.65	7.630	5.65±0.04	5.46±0.05	0.37±0.18
Benzene	1.91	0.603	5.82±0.07	5.41±0.05	0.68±0.20
Toluene	2.27	0.552	5.68±0.06	5.15±0.06	0.80±0.18
Xylene	2.39	0.605	5.61±0.05	5.13±0.06	0.70±0.16
Carbon tetrachloride	2.59	0.904	5.22±0.05	4.91±0.05	0.47±0.15

that the very efficient transfer of excitation energy within the Chl *a* monomer ensemble, even in only moderately concentrated solutions, will enhance markedly the quenching of the Chl *a* monomer fluorescence by ground state dimers.

The dependence of the fluorescence decay of Chl *a* on the concentration is a function of the solvent. For instance, the fluorescence lifetimes of Chl *a* at a concentration of 1.0 mM in benzene and carbon tetrachloride are 4.56±0.08 ns and 4.10±0.03 ns respectively, both values being significantly shorter than those measured at 0.1 μM in these solvents (see Table 1). It has been established [24] that Chl *a* dimerizes in non-polar solvents with a dimerization constant greater than that in polar solvents, and hence the decrease in the fluorescence lifetimes observed in benzene and carbon tetrachloride at 1.0 mM can be attributed to the quenching of fluorescence from monomeric Chl *a* by dimers.

3.2. Quenching of Chl a fluorescence by oxygen in bulk solution

3.2.1. Dilute solutions

Oxygen quenches the fluorescence from Chl *a* efficiently. The energy levels of S_1 and T_1 for Chl *a* can be estimated from the absorption and phosphorescence band origins [25,26]. The energy gap between S_1 and T_1 is calculated to be no more than 5000 cm^{-1}, and hence is not sufficiently large to produce singlet oxygen ($^1\Delta_g$=7800 cm^{-1}), which would result if the fluorescence quenching reaction proceeded via spin-allowed energy transfer to the oxygen molecule in the ground state ($^3\Sigma_g^-$) [1,27,28]. Thus the process given by Eq. (3) is eliminated from the quenching mechanism on the basis of energetic considerations

$$S_1 + O_2(^3\Sigma_g^-) \rightarrow T_1 + O_2(^1\Delta_g) \quad (3)$$

Another conceivable spin-allowed quenching process is given by Eq. (4)

$$S_1 + O_2(^3\Sigma_g^-) \rightarrow T_1 + O_2(^3\Sigma_g^-) \quad (4)$$

The quenched fluorescence decay curves measured for Chl *a* in dilute aerated solutions can be described adequately by a single-exponential function. The rate constant for the quenching of the fluorescence by oxygen (k_q) can be calculated using Eq. (5)

$$1/\tau_q - 1/\tau_0 = k_q[O_2] \quad (5)$$

where τ_0 and τ_q are the unquenched and quenched fluorescence lifetimes of Chl *a* in solution respectively. The values for k_q were determined for Chl *a* in a wide range of solvents and are summarized in Table 1, together with the values for τ_0 and τ_q. The values for k_q are all significantly smaller than the value for k_{diff}, the rate constant for a diffusion-controlled bimolecular reaction, calculated using Eq. (6), where η is the solvent viscosity

$$k_{diff} = 8RT/2\eta \quad (6)$$

The logarithmic values of k_q obtained for alcoholic solvents containing a Chl *a* concentration of 0.1 μM are plotted in Fig. 4 as a function of the logarithmic values of the solvent viscosity. The dependence of k_q on η can be described phenomenologically by Eq. (7) [4]

$$k_q = A\eta^{-\alpha} \quad (7)$$

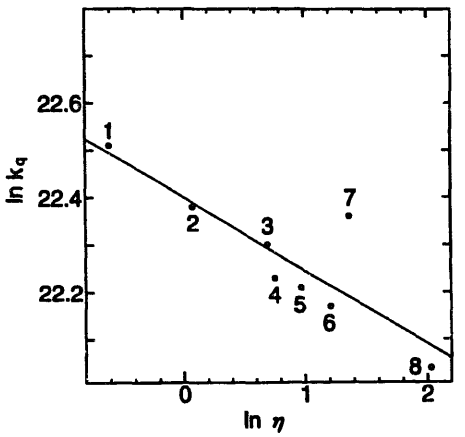

Fig. 4. Dependence of k_q on viscosity observed in alcoholic solvents at 298 K at a concentration of 0.1 μM: 1, methanol; 2, ethanol; 3, 2-propanol; 4, 1-propanol; 5, *n*-butanol; 6, *n*-pentanol; 7, 2-methyl-1-propanol; 8, *n*-octanol.

Table 2
Concentration dependence of the rate constant of fluorescence quenching by oxygen for Chl *a* in *n*-octanol

Chl *a* (mM)	τ_0 (ns)	τ_q (ns)	k_q (10^{10} M^{-1} s^{-1})
0.0001	5.65±0.04	5.46±0.05	0.37±0.18
1.0	5.65±0.05	5.03±0.04	1.3±0.2
5.0	5.42±0.05	4.80±0.06	1.4±0.3
7.5	4.87±0.05	4.43±0.05	1.2±0.3
10	4.50±0.05	4.02±0.04	1.6±0.3
25	2.82±0.03	2.58±0.03	2.0±0.5

A good straight line is obtained for a Chl *a* concentration of 0.1 μM and the value of the exponent α in Eq. (7) is 0.18. The dependence of k_q on η found for Chl *a* is similar to that for anthracene [5] and 9,10-dimethylanthracene [29] in alcoholic solvents. However, the values for k_q obtained experimentally are smaller than those predicted by Eq. (6) for fully diffusion-controlled reactions. Therefore, over the viscosity range examined in this work, the quenching of Chl *a* fluorescence by oxygen does not appear to be governed solely by material diffusion but may involve an activated process [4,30,31].

3.2.2. Concentrated solutions

Both the quenched and unquenched fluorescence decays for the concentrated solutions can be described well by a single-exponential function provided that the Chl *a* concentration is not higher than 50 mM. The values of k_q evaluated using Eq. (5) for several concentrations of Chl *a* in *n*-octanol are listed in Table 2. These values display an increase with increasing Chl *a* concentration. The value of k_q at a Chl *a* concentration of 25 mM ($(2.0\pm0.5)\times10^{10}$ M^{-1} s^{-1}) is approximately five times larger than that obtained for the dilute solution. Energy migration, which is more efficient at higher concentrations, is believed to be responsible for the increase in the value of k_q with increasing Chl *a* concentration.

It is not difficult to explain qualitatively the reason for the increase in the values of k_q observed on increasing the concentration of Chl *a* in the bulk solution. Excitation energy migration among Chl *a* molecules, which is mediated by dipole–dipole Förster-type interactions [32], becomes more efficient with increasing concentration of Chl *a* because the average intermolecular distance between two Chl *a* molecules becomes shorter. This leads to the enhancement of the probability of an excited molecule being in the vicinity of an oxygen molecule, thereby resulting in a significant increase in the apparent quenching rate constant. Thus the rate constant for a fluorescence quenching reaction mediated solely by material diffusion in dilute solution can be modified in concentrated solution due to rapid energy migration among the fluorophores. The values of k_q are larger at higher Chl *a* concentrations than at lower concentrations for all of the alcoholic solvents used in this work.

It should be emphasized here that, if the effects of re-absorption are not removed, the apparent fluorescence lifetime increases with increasing concentration, without being accompanied by any apparent deviation from single exponentiality under certain circumstances [14,33]. The increase in the apparent lifetime as a result of re-absorption would be expected to be greater for deaerated solutions than for aerated solutions for a given concentration of a fluorophore because the probability of re-absorption is higher the larger the fluorescence quantum yield. As a result of this, the apparent quenching rate constant, calculated by substituting these distorted apparent lifetimes into Eq. (5), increases as the distortion becomes more significant with increasing concentration [33]. This type of superficial effect of concentration on the k_q values is absent in the present work. The values of k_q reported for Chl *a* [34] and many other organic molecules [35] are larger than those obtained for dilute solutions simply because of this re-absorption effect.

3.3. Quenching of Chl a fluorescence by oxygen in microdroplets

It has been reported previously [12] that the decay of fluorescence from ethylene glycol microdroplets containing high concentrations of rhodamine B exhibits a dependence on the droplet size. Recently, a significant dependence on the droplet size of the fluorescence decay features of R6G at high concentrations (1.0–5.2 mM) and the energy transfer from R6G (0.10 mM) to malachite green (0.75 mM) has been observed [36].

Fig. 5 shows the fluorescence decay curves measured for 10 μm diameter aerated and deaerated droplets of *n*-octanol containing a Chl *a* concentration of 1.0 mM. The fluorescence

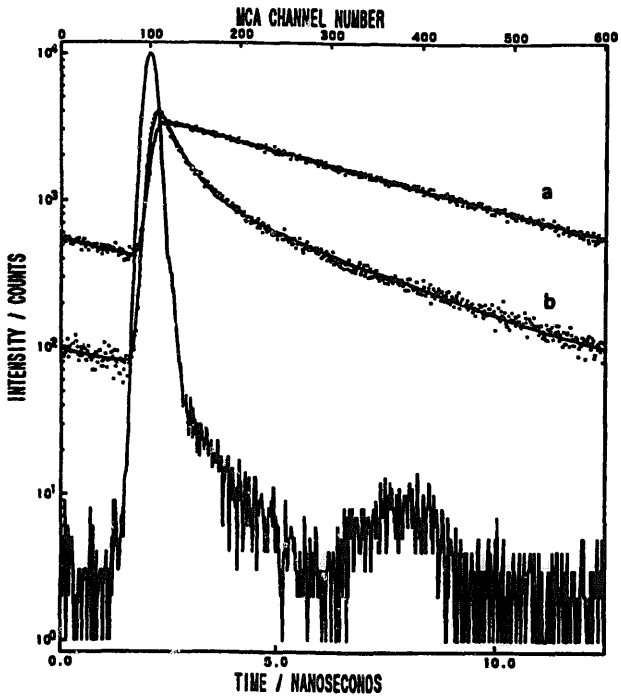

Fig. 5. Fluorescence decay curves measured for degassed and aerated droplets of *n*-octanol containing Chl *a* dispersed in water: (a) degassed droplet; (b) aerated droplet. The droplet size is 10 μm.

decay curves measured for the deaerated droplets can be fitted satisfactorily using a single-exponential function, irrespective of the droplet size, provided that prolonged laser irradiation is avoided by restricting the maximum counts at the peak intensity of the fluorescence decay curve to less than 2×10^3. The fluorescence lifetimes obtained for the deaerated droplets are denoted by τ_0^D.

The values obtained for τ_0^D at four different concentrations of Chl *a* over a range of droplet sizes are listed in Table 3. The value of τ_0^D at a Chl *a* concentration of 0.1 mM is essentially independent of the droplet size, indicating that neither intramolecular radiative nor intramolecular non-radiative processes are influenced by the droplet size under the present experimental conditions. However, at higher concentrations of Chl *a*, the values of τ_0^D decrease as the diameter of the droplet decreases, the dependence of τ_0^D on size being larger for the droplets containing higher concentrations of Chl *a*.

The fluorescence decay curves measured for the aerated droplets deviate significantly from exponentiality and so were analysed using a sum of two exponentials. This deviation from exponentiality is attributed to the photodegradation of Chl *a* [37], and is far more extensive in the droplets than in bulk solution. The chronological change in the decay curve observed on laser irradiation is shown in Fig. 6. The lifetimes associated with the two fluorescence decay components remain unchanged on irradiation, but the fractional contributions of these two components to the total fluorescence vary such that the fraction of the shorter lived component (approximately 330 ps) increases with increasing time of irradiation. Therefore this component is ascribed to fluorescence from an unidentified photoproduct and the longer lived component to the fluorescence from Chl *a* quenched by oxygen.

The values of the net rate constant for fluorescence quenching in the droplets (k_q^D) were calculated using Eq. (8)

$$1/\tau_q^D - 1/\tau_0^D = k_q^D[O_2] \quad (8)$$

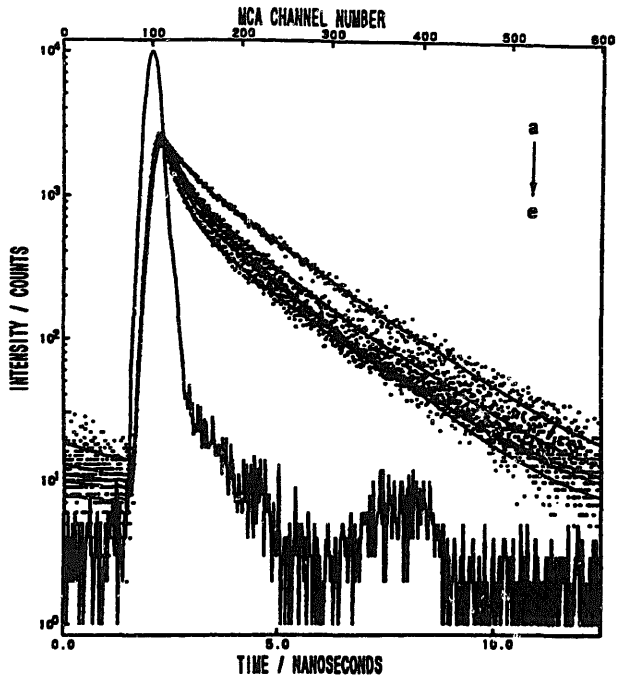

Fig. 6. Effect of laser irradiation on the fluorescence decay features of Chl *a* in a droplet of *n*-octanol (initial Chl *a* concentration, 5 mM): (a) 200 s; (b) 400 s; (c) 1000 s; (d) 1600 s; (e) 2200 s. The two component lifetimes remain constant and only the fractions of the components vary with irradiation.

where τ_0^D and τ_q^D are the fluorescence lifetimes of a deaerated droplet and of the longer lived component of the double-exponential fluorescence decay obtained for an aerated droplet of the same diameter respectively. The values calculated for k_q^D are summarized in Table 3 and display a clear dependence on the droplet size. The largest value of k_q^D, $(85\pm12)\times10^{10}\ M^{-1}\ s^{-1}$, was obtained for a droplet of 4 μm in diameter containing a Chl *a* concentration of 30 mM. This value of k_q^D is some 230 times greater than the value obtained for the dilute solution of Chl *a* (see Table 1). In fact, to our knowledge, this value is the largest ever reported

Table 3
Rate constants of fluorescence quenching by oxygen of Chl *a* in *n*-octanol droplets dispersed in water as a function of the droplet size

Diameter (μm)	τ_0^D (ns)	τ_q^D (ns)	k_q^D (10^{10} M^{-1} s^{-1})	Diameter (μm)	τ_0^D (ns)	τ_q^D (ns)	k_q^D (10^{10} M^{-1} s^{-1})
[Chl *a*] = 0.1 mM				[Chl *a*] = 5.0 mM			
5	5.39±0.12	4.11±0.27	3.6±1.2	4	3.05±0.15	2.37±0.15	5.8±2.6
6	5.42±0.12	4.29±0.26	3.0±1.1	8	3.14±0.11	2.52±0.15	4.8±2.1
8	5.55±0.12	4.17±0.26	3.7±1.2	12	3.40±0.13	2.73±0.17	4.4±2.1
10	5.35±0.12	4.24±0.27	3.0±1.2	16	4.29±0.14	3.52±0.21	3.1±1.5
15	5.57±0.12	4.55±0.23	2.5±0.9	20	4.42±0.15	3.85±0.15	2.0±1.1
20	5.50±0.12	4.80±0.21	1.6±0.8	24	4.54±0.16	4.14±0.20	1.5±1.2
27	5.58±0.12	5.03±0.21	1.2±0.7	28	4.87±0.16	4.32±0.19	1.6±1.0
[Chl *a*] = 10 mM				[Chl *a*] = 30 mM			
4	3.02±015	2.18±0.08	7.7±2.0	4	1.45±0.06	0.48±0.04	85±12
8	3.17±0.20	2.24±0.08	7.9±2.2	8	1.49±0.06	0.50±0.04	81±11
12	3.13±0.14	2.47±0.08	5.2±1.7	12	1.54±0.06	0.53±0.04	76±10
16	3.37±0.16	2.70±0.09	4.4±1.6	16	1.99±0.07	0.67±0.03	60±5
20	3.40±0.14	2.95±0.10	2.7±1.4	20	2.09±0.07	0.95±0.04	35±4
24	3.50±0.15	3.09±0.10	2.3±1.4	24	2.25±0.08	1.06±0.04	30±3
28	3.74±0.15	3.35±0.08	1.9±1.1	28	2.44±0.08	1.16±0.04	27±3

for the fluorescence quenching by oxygen in solution [1–4,19,23,35], and far exceeds the value of k_{diff} calculated using Eq. (6). The possibility that the concentration of oxygen in the droplet increases greatly when the concentration of Chl *a* is increased was eliminated by comparing the concentrations of oxygen in the most concentrated and most dilute solutions by gas chromatography. Furthermore, the concentration of oxygen in an *n*-octanol solution saturated with water was found to be practically the same as that in a pure *n*-octanol solution. Therefore it is very unlikely that the concentration of oxygen in small droplets is many times higher than that in the bulk solution of *n*-octanol, although the concentration of oxygen in the droplets could not be measured directly. Thus the large increase in the quenching rate constant in the droplet is not the result of a significant change in the concentration of oxygen.

The reduction in the fluorescence decay time (τ_0^D) with decreasing droplet diameter for Chl *a* concentrations greater than 0.1 mM, as shown in Table 3, indicates that either the efficiency of energy migration among the Chl *a* monomers is enhanced when the Chl *a* molecules are confined in smaller droplets, leading to more pronounced quenching by ground state Chl *a* dimers, or that the concentration of the non-emissive dimer increases with decreasing droplet size. The latter possibility can be eliminated because this would be expected to result in a reduction in the efficiency of fluorescence quenching by oxygen for smaller droplets. Inspection of the data in Table 3 reveals that this is not the case.

A significantly higher efficiency of Förster-type non-radiative energy transfer from coumarin-1 to R6G contained in levitated 10 μm diameter glycerol microdroplets compared with that in bulk glycerol has been reported previously [38]. It was shown [38–40] that this phenomenon results from the mediation of the dipole–dipole interaction by morphology-dependent resonances (MDRs) of the particle. Furthermore, the dependence on the droplet diameter of the fluorescence lifetime of dilute solutions of R6G in levitated glycerol and ethylene glycol microdroplets has been reported recently [41–43]. This was attributed [41] to a greater proportion of the fluorophores being able to interact with a cavity mode of the MDR in the smaller droplets as a result of the relative increase in mode volume with decreasing droplet diameter. A similar dependence of the luminescence lifetime on the droplet size has also been observed for chelated europium ions in dimethylformamide–alcohol microdroplets [44]. In the present case, however, there is a much smaller difference in the refractive index between the droplet and the surrounding medium. Therefore, as the condition for the enhancement of energy transfer by MDR is barely satisfied, it is unlikely that the observed effect results from the influence of MDR. Although we are unable to provide any theoretical rationalization for the observed effects, it is proposed that the reduction in τ_0^D with decreasing droplet diameter for droplets containing Chl *a* in excess of 0.1 mM, observed in the present work, arises predominantly from the progressive enhancement of the rate of non-radiative energy migration among Chl *a* monomers. This results in more efficient trapping of the available excitation energy by non-emissive dimers, leading to lower values of τ_0^D. For the same reasons, the probability of the trapping of excitation energy by oxygen molecules also increases, resulting in an increasing magnitude of k_q^D with decreasing droplet diameter. A similar many-fold enhancement in the efficiency of Förster-type energy transfer with decreasing droplet diameter has also been observed recently [36] for droplets containing R6G and malachite green.

Heterogeneity in the quencher distribution in small droplets may cause some unusual phenomena. In the present case, oxygen is not expected to be distributed inhomogeneously in the droplets since the solubility of oxygen differs little between water and *n*-octanol. Although heterogeneity in the distribution of Chl *a* is possible, particularly near the surface of the droplets [45], no evidence for this was found in the present work.

4. Conclusions

The quenching of Chl *a* fluorescence by oxygen in highly concentrated solutions in both bulk solution and in microdroplets has been investigated. The rate constant of fluorescence quenching by oxygen in bulk solutions (k_q) increases with increasing Chl *a* concentration. This is ascribed to enhanced excitation energy migration among monomeric Chl *a* molecules, resulting from the reduction in their mean separation distance with increasing Chl *a* concentration. The values of k_q for dilute solutions of Chl *a* in alcoholic solvents display a fractional power dependence on the solvent viscosity which is typical for reactions proceeding at rates lower than that associated with material diffusion.

The net rate constant for fluorescence quenching by oxygen in microdroplets (k_q^D) displays a significant increase with decreasing droplet diameter for Chl *a* concentrations greater than 0.1 mM. The value of k_q^D at a Chl *a* concentration of 30 mM in a 4 μm diameter droplet of $85 \times 10^{10}\,M^{-1}\,s^{-1}$ is some 230 times larger than the value of k_q in dilute solution. This extremely large value of k_q^D is proposed to arise from the enhanced migration of excitation energy within the Chl *a* monomer ensemble.

Little is known about the role of oxygen as a quencher of the light energy absorbed by chloroplasts [46]. However, the effect of droplet size on k_q^D observed in this work suggests that there may exist an optimum chloroplast size at which the probability of trapping of the migrating excitation energy at the so-called "special pair" in photosystem II (PSII) exceeds significantly that of the trapping by oxygen produced in PSII as a result of the oxidation of water [6]. The enhancement of the fluorescence quenching by oxygen observed for the microdroplets is also relevant to the interpretation of the fluorescence decay curves measured for extracted photosynthetic organelles under aerated conditions [47]. At present, however, further work is required in order to establish whether the presence of oxygen modifies the decay features

of fluorescence from Chl *a* in single photosynthetic organisms, such as *Euglena gracilis* Z [48] or *Chlamydomonas* [49], isolated photosynthetic particles [50] or reaction centres in the extracted thylakoid membranes [51].

Acknowledgements

S.H. is grateful for financial support from the Japanese Government Ministry of Education, Science and Culture (Grants-in-Aid nos. 04215103 and 03640407). A.D.S. expresses appreciation for financial support from a JSPS Postdoctoral Fellowship during his stay at the Kyoto Institute of Technology.

References

[1] J. Saltiel, B.M. Atwater, in: G.S. Hammond (Ed.), Advances in Photochemistry, vol. 14, Wiley-Interscience, New York, 1987.
[2] I.B. Berlman, Handbook of Fluorescence Spectra of Aromatic Molecules, Academic Press, New York, 1965, p. 37.
[3] H. Yasuda, A.D. Scully, S. Hirayama, M. Okamoto, F. Tanaka, J. Am. Chem. Soc. 112 (1990) 6847.
[4] S. Hirayama, H. Yasuda, A.D. Scully, M. Okamoto, J. Phys. Chem. 98 (1994) 4609.
[5] K.K. Pandey, M. Okamoto, S. Hirayama, Chem. Phys. Lett. 224 (1994) 417.
[6] Govindjee, W.J. Coleman, Sci. Am. 262 (2) (1990) 42.
[7] A. Penzkofer, Y. Lu, Chem. Phys. 103 (1986) 399.
[8] A.D. Scully, M. Matsumoto, S. Hirayama, Chem. Phys. 157 (1991) 253.
[9] C. Bojarski, Z. Naturforsch. 37 (1982) 150.
[10] D.W. Lawlor, Photosynthesis: Molecular, Physiological and Environmental Processes, 2nd ed., Longman Scientific and Technical, 1993, Chapter 4.
[11] B. Nathanson, J.E. White, Plant. Physiol. 59 (1974) 196.
[12] M. Kawahigashi, S. Hirayama, J. Lumin. 43 (1989) 207.
[13] S. Hirayama, in: J.F. Rabek (Ed.), Progress in Photochemistry and Photophysics, vol. VI, CRC Press, 1992, p. 1.
[14] T. Minami, M. Kawahigashi, Y. Sakai, K. Shimamoto, S. Hirayama, J. Lumin. 35 (1986) 247.
[15] H.K. Lichtenthaler, Methods Enzymol. 148 (1987) 350.
[16] K. Nakamura, MSc Thesis, Kyoto Institute of Technology, 1994.
[17] R. Aoshima, T. Chiba, H. Asai, Appl. Opt. 23 (1984) 597.
[18] T. Taguchi, S. Hirayama, M. Okamoto, Chem. Phys. Lett. 231 (1994) 561.
[19] S.L. Murov, Handbook of Photochemistry, 2nd ed., Marcel Dekker, 1993.
[20] G.S. Beddard, G. Porter, Nature 260 (1976) 366.
[21] J. Dalton, J. Chem. Soc., Chem. Commun. (1980) 78.
[22] R.F. Loring, H.C. Anderson, M.D. Fayer, J. Chem. Phys. 76 (1982) 2015.
[23] D.P. Miller, R.J. Robbins, A.H. Zewail, J. Chem. Phys. 75 (1981) 3649.
[24] J.J. Katz, L.L. Shipman, T.M. Cotton, T.R. Janson, in: D. Dolphin (Ed.), The Porphyrins, vol. V, part C, Academic Press, New York, 1978, pp. 401–458.
[25] J.C. Scaiano, Handbook of Organic Photochemistry, vols. I and II, CRC Press, 1987.
[26] A.J. Hoff, in: Govindjee, J. Amesz, D.C. Fork (Eds.), Light Emission by Plants and Bacteria, Academic Press, New York, 1986.
[27] F. Wilkinson, D.J. McGarvey, A.F. Olea, J. Am. Chem. Soc. 115 (1993) 12 144.
[28] Y. Usui, N. Shimizu, S. Mori, Bull. Chem. Soc. Jpn. 65 (1992) 897.
[29] W.R. Ware, J. Phys. Chem. 66 (1962) 455.
[30] S.A. Rice, in: C.H. Bamford, C.F.H. Triper, R.G. Compton (Eds.), Comprehensive Chemical Kinetics, vol. 25, Diffusion-Limited Reactions, Elsevier, Amsterdam, 1985.
[31] A.D. Scully, T. Takeda, M. Okamoto, S. Hirayama, Chem. Phys. 228 (1994) 32
[32] Th. Förster, Z. Naturforsch., Teil A 4 (1949) 321.
[33] M. Kaplanova, K. Cermak, J. Photochem. 15 (1980) 313. S.A. El-Daly, M. Okamoto, S. Hirayama, J. Photochem. Photobiol. A: Chem. 91 (1995) 105.
[34] J.S. Connolly, J. Frederick, E.B. Samuel, Photochem. Photobiol. 36 (1982) 559.
[35] Landolt-Börnstein Gruppe II Band 3 Luminezenz Organisher Substanzen, Springer-Verlag, Berlin, 1967, p. 300.
[36] K.K. Pandey, S. Hirayama, J. Photochem. Photobiol. A: Chem. 99 (1996) 165.
[37] M.N. Merzlyak, S.I. Pogosyan, L. Lekhimena, T.V. Zhigalova, I.F. Khozina, Z. Cohen, S.S. Khrushchev, Russ. J. Plant Physiol. 43 (1996) 160.
[38] L.M. Folan, S. Arnold, S.D. Druger, Chem. Phys. Lett. 118 (1985) 322.
[39] S.D. Druger, S. Arnold, L.M. Folan, J. Chem. Phys. 87 (1987) 2649.
[40] S. Arnold, L.M. Folan, Opt. Lett. 14 (1989) 387.
[41] M.D. Barnes, W.B. Whitten, S. Arnold, J.M. Ramsey, J. Chem. Phys. 97 (1992) 7842.
[42] M.D. Barnes, W.B. Whitten, J.M. Ramsey, J. Opt. Soc. Am. B 11 (1994) 1297.
[43] M.D. Barnes, W.B. Whitten, J.M. Ramsey, Chem. Phys. Lett. 227 (1995) 628.
[44] H.-B. Lin, J.D. Eversole, C.D. Merritt, A.J. Campillo, Phys. Rev. A. 45 (1992) 6756.
[45] H. Yao, Y. Inoue, H. Ikeda, K. Nakatani, H.-B. Kim, N. Kitamura, J. Phys. Chem. 100 (1996) 1494.
[46] Y. Qin, Y. Zuokun, Yingyong Huaxue 1 (1983) 108; Chem. Abstr. 101 (1983) 188255t.
[47] I. Moya, P. Sebban, W. Haehnel, in: J. Amesz, D.C. Fork (Eds.), Light Emission by Plants and Bacteria, Academic Press, New York, 1986.
[48] S. Hirayama et al., to be published.
[49] R.T. Gulotty, L. Mets, R.S. Albert, G.R. Fleming, Photochem. Photobiol. 41 (1985) 487.
[50] G.H. Shatz, H. Brock, A.R. Holtzworth, Proc. Natl. Acad. Sci. USA 84 (1987) 8414.
[51] R.C. Dunn, G.R. Holtom, L. Mets, X.S. Xie, J. Phys. Chem. 89 (1994) 3094.